Talanta 82 (2010) 1980–1985

Contents lists available at ScienceDirect

Talanta

journal homepage: www.elsevier.com/locate/talanta

Electrochemical study of gelatin as a matrix for the immobilization of horse heart cytochrome *c*

Karolien De Wael[a,*,1], Stijn De Belder[a], Sandra Van Vlierberghe[b,1], Geert Van Steenberge[c], Peter Dubruel[b], Annemie Adriaens[a]

[a] Department of Analytical Chemistry, Ghent University, Krijgslaan 281 S12, B-9000 Ghent, Belgium
[b] Polymer Chemistry & Biomaterials Research Group, Ghent University, Krijgslaan 281 S4-Bis, B-9000 Ghent, Belgium
[c] Department of Electronics and Information Systems, Centre for Microsystems Technology, Ghent University, Technologiepark 914A, B-9052 Ghent, Belgium

ARTICLE INFO

Article history:
Received 10 June 2010
Received in revised form 6 August 2010
Accepted 17 August 2010
Available online 24 August 2010

Keywords:
Cytochrome *c*
Gelatin
Hydrogel
ATR-IR spectroscopy
Surface profilometry
Bioelectrochemistry

ABSTRACT

The aim of this paper is to emphasize the strength of gelatin as a stable matrix for redox enzymes. Cyclic voltammetry has been applied for a detailed electrochemical study of horse heart cytochrome *c* (HHC) entrapped in a gelatin matrix immobilized on a gold electrode. The influence of the HHC concentration, the mass percentage of the gelatin and the nature of the gelatin on the electrochemical behaviour of HHC have been described in detail. In addition, attenuated total reflection infrared (ATR-IR) spectroscopy was used to prove the immobilization on a qualitative and conformational level. The thickness of the gelatin film was determined using a non-contact optical profiler. These results open up new perspectives in the development of stable, biocompatible matrices for redox enzymes. The latter has its relevance in the field of biosensor development.

1. Introduction

Protein film formation by cross-linking and the incorporation of enzymes in hydrogels, adsorbed to electrode surfaces, are new and innovating aspects in the field of bioelectrochemistry. Both offer new perspectives in the development of stable biosensors. In this work we will address the second route. Different types of gelatin will be selected as a possible hydrogel for the encapsulation of proteins or enzymes. Gelatin is a water soluble protein, composed of a variety of amino acids [1], via amide bonds forming a linear polymer with a molecular weight between 15,000 and 250,000 Da [2]. This hydrophilic polymer network is able to swell in water by absorbing a large amount of water (one tenth to one thousand times their dry weight) [3]. Due to the hydrophilic groups or domains, the hydration and native configuration of the encapsulated biomolecules is ensured. Because of the high degree of swelling in water, hydrogels possess other desired characteristics such as the rapid diffusion of the substrate of the enzyme and the formed reaction product. Otherwise, there is often an increased enzyme stability and an increased mobility of the counter ions, which is important for fast charge transfer reactions. A gelatin hydrogel is thus a (cross-linked) three-dimensional hydrophilic polymer network, which can provide a desirable water-rich buffering environment for the entrapped proteins because of its attractive properties of film-forming ability, biocompatibility, non-toxicity, high mechanical strength and cheapness. Different types of gelatin can be distinguished according to their production process [4]. Type A gelatin which possesses an iso-electric point (IEP) of 6–8 is obtained by acidic hydrolysis of collagen. Type B gelatin (IEP 4.7–5.3) is produced by an alkaline treatment of collagen. Type B gelatin differs from type A by the hydrolysis of the amide groups. By this amidolysis, aspartine and glutamine are converted to aspartic acid and glutamic acid. The extra acid groups reduce the IEP of type B gelatin. Also arginine can be hydrolyzed to ornithine in alkaline conditions [5]. In addition to triple helix formation (i.e. physical cross-linking) which occurs below the gelation temperature (ca. 35 °C), a chemical cross-linking step can also be introduced. In the present work, two gelatin derivatives (i.e. thiolated and methacrylamide-modified) were applied and compared as an embedding matrix.

Cytochrome *c* plays an important role in the biological respiratory chain, receiving electrons from cytochrome *c* reductase and delivering them to cytochrome *c* oxidase [6,7]. The crucial role of cytochrome *c* in the respiratory chain of mitochondria has inspired scientists to study the mechanism of the electron transfer process. The study of the electrochemistry of cytochrome *c* is thus of high

* Corresponding author. Tel.: +32 9 264 48 20; fax: +32 9 264 49 60.
E-mail address: Karolien.DeWael@UGent.be (K. De Wael).
[1] Postdoctoral Fellow of the Research Foundation - Flanders (Belgium).

0039-9140/$ – see front matter © 2010 Elsevier B.V. All rights reserved.
doi:10.1016/j.talanta.2010.08.019

relevance. In this work, horse heart cytochrome *c* (HHC) was chosen as redox protein as it has been studied extensively with respect to direct protein electrochemistry (see [8–10] and references therein) and has often been considered as a model system for biological electron transfer [11] and for bioelectrocatalysis [12].

In this work, HHC is encapsulated into the selected types of gelatin using the drop drying technique after which the electrochemical behaviour of HHC in a gelatin matrix is investigated. As far as the authors are aware, there is no literature with respect to the entrapment of HHC in a gelatine matrix. The influence of the HHC concentration, mass percentage of the gelatin and the nature of the gelatin is described in detail. In addition, attenuated total reflection infrared (ATR-IR) spectroscopy is used to prove the immobilization on a qualitative and conformational level. The thickness of the gelatin film was determined using a non-contact optical profiler.

These parameters are important with respect to biosensor applications since, in future work specialty enzymes and/or proteins will be incorporated in the HHC film to enable monitoring certain biochemical and/or physiological changes. As a result, a profound understanding of the characteristics of the HHC film deposited on the electrode surface is essential. These results will be used as stepping stone for immobilizing different types of enzymes in a similar manner, thereby reaching other applications (e.g. the immobilization of cytochrome *c* peroxidase for the reduction of hydrogen peroxide). Different target molecules and their analytical concentrations will be detected by using these types of sensor systems.

2. Materials and methods

2.1. Chemicals and solutions

Horse heart cytochrome *c* (HHC), 2-[4-(2-hydroxyethyl)-piperazinyl]ethanesulfonic acid (HEPES), mercaptohexanol (MH) and sodium hydroxide were purchased from Sigma-Aldrich. Potassium ferrocyanide ($K_4Fe(CN)_6$) was purchased from Merck Eurolab. The HEPES buffer solution of 10×10^{-3} mol L^{-1} was set to pH 7.0 using a 0.15 mol L^{-1} NaOH solution. Type B gelatin (IEP = 5, Bloom strength = 257), isolated from bovine skin by the alkaline process, was kindly supplied by SKW Biosystems (Ghent, Belgium). Type A gelatin (IEP = 8.8, Bloom strength = 202), isolated from porcine skin by the acid treatment, was obtained from Rousselot (Ghent, Belgium). Methacrylic anhydride (MAA) was purchased from Aldrich (Bornem, Belgium) and was used as received. Type B gelatin was chemically modified with methacrylamide side groups, resulting in a degree of substitution (DS) of 60%, as described in a previous paper [13]. The methacrylamide-modified gelatin is further referred to as GelMOD. The thiolated gelatin (GelSH) was synthesized as described previously [14]. In brief, the amines of type B gelatin were modified with N-acetyl-homocysteine thiolactone (5 equiv., 1.51 g) (Acros). After stirring for 3 h at 40 °C, GelSH was purified and isolated using lyophilization. The degree of substitution of GelSH was 65%.

2.2. Electrode preparation

Electrochemical experiments were performed in a three electrode cell using a saturated calomel reference electrode (SCE) containing two compartments (Radiometer Analytical, France) and a platinum counter electrode. The working electrodes were gold electrodes with a diameter of 1.6 mm (BAS, UK) which were pretreated by mechanical and electrochemical polishing according to the following procedure. Before its first use the electrode surface was briefly scoured by a silicon carbide emery paper of 1200 grit to obtain a fresh surface. To smoothen the resulting relatively rough surface it was further subjected to sequential polishing by polishing cloth covered with alumina powder of 1, 0.3 and 0.05 mm particle size (Buehler, USA) for respectively 5, 10 and 20 min. To remove any adherent Al_2O_3 particles the electrode surface was rinsed thoroughly with doubly deionised water and cleaned in an ultrasonic bath containing deionised water (Branson 3210, USA) for 2 min.

Before immobilizing gelatin onto the electrode, the gold surface was modified with a self-assembled monolayer (SAM) of 6-mercaptohexanol (unless otherwise indicated). The latter was done by immersing the electrode in a water solution containing 1 mmol L^{-1} 6-mercaptohexanol (MH) for 18 h at room temperature. The modified gold electrodes were consequently rinsed with water to remove any physically adsorbed mercaptohexanol. In what follows, these modified electrodes are denoted as MH|Au.

To immobilize gelatin onto a MH|Au electrode or bare Au, 7 μL of a gelatin solution (5, w/v%) was brought onto the surface by using a syringe and was exposed to air for 2 h at 4 °C (drop drying). The gelatin solution was prepared by mixing the gelatin powder and the HEPES buffer solution at 40 °C. These electrodes are referred to in the text as Gel|MH|Au. When HHC was added to the gelatin-HEPES solution, the electrodes are denoted as HHC|Gel|MH|Au. Finally, all electrodes were washed with the HEPES buffer solution and stored at 4 °C before use. Unless stated otherwise, the concentration of HHC and gelatin was respectively 0.14 mmol L^{-1} and 5 (w/v)%.

2.3. Apparatus

A PGSTAT20 potentiostat controlled by GPES 4.9 005 software package running (ECO Chemie, The Netherlands) was used to record voltammetric curves. Prior the start of each measurement, the pH of the solution was measured using an Orion Benchtop pH-meter model 420A (Thermo Fisher Scientific, USA). The solutions were thoroughly deoxygenated by bubbling nitrogen through the cell solution for 20 min and a nitrogen atmosphere was maintained over the solution during the experiment.

ATR-IR spectroscopic analyses were performed in order to obtain qualitative proof of the immobilization of HHC onto the gelatine modified metal surface. Transmittance spectra were acquired using a Biorad FT-IR spectrometer FTS 575C equipped with a 'Golden Gate' ATR accessory. The latter was fitted with a diamond crystal. The coating covering the electrode surface was measured directly by pressing the electrode against the ATR crystal. The spectra were recorded over the range 4000–600 cm^{-1} and averaged over 16 scans.

The surface profile of the samples were measured with a Wyko NT3300 non-contact optical profiler. The thickness of semi-transparent films can be obtained by measuring a step or by measuring through the film to the substrate. In the latter case, the VSI technique is employed. In VSI, the optical system is translated vertically such that the upper and lower film surfaces pass through focus. For each location in the field of view, two sets of interference fringes develop during the scan: one corresponding to best focus at the air/film interface, the second corresponding to the film/substrate interface. Thick Film Analysis, a Vision software option, determines thickness based on these fringes. The analysis first determines the vertical centers of the two fringe envelopes then calculates the distance between their centers. This distance is divided by the film's index of refraction to determine its thickness. A second approach for determining the thickness by the optical profiler is making a gap in the gelatin film with a CO_2 laser and measuring the thickness of the film at the edge. The CO_2 laser (GSIL Impact SSM 2150) operates in the 9–10 μm range. The maximum optical power is 60 W, corresponding to a maximum pulse energy of 0.4 J, and a maximum pulse repetition rate of 150 Hz. The pulse length is 70 nsec.

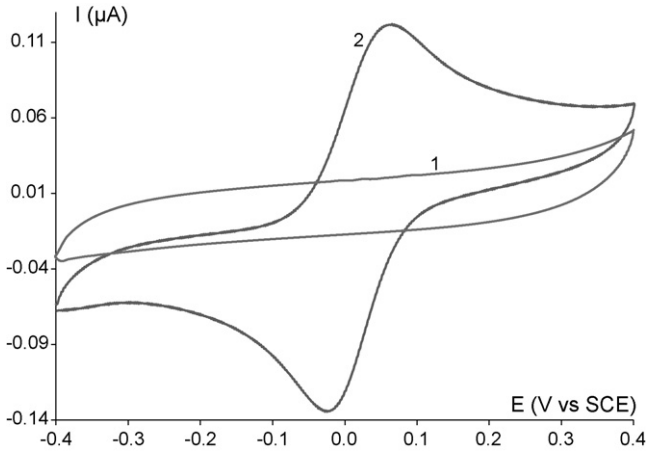

Fig. 1. The current potential behaviour of a GelB(5 m%)|MH|Au electrode (1) and a HHC(0.14 mM)|GelB(5 m%)|MH|Au electrode (2) in a 10 mmol L^{-1} HEPES pH 7 buffer solution with a scan rate of 50 mV s^{-1}.

3. Results and discussion

3.1. Electrochemical detection of HHC in a gelatin B matrix

Curve 1 in Fig. 1 shows the electrochemical response of a GelB|MH|Au electrode in a 10 mmol L^{-1} HEPES pH 7 buffer solution in a potential window from −0.4 V versus 0.4 V with a scan rate of 50 mV s^{-1}. Not any oxidation or reduction process could be observed in this specific potential window. For this reason, we consider the polymeric gelatin matrix very suitable for bioelectrochemistry as it has no electrochemical background signal in the potential range in which protein electrochemistry takes place [15–16].

When 0.14 mmol L^{-1} HHC is added to the GelB matrix, the corresponding current potential behaviour is shown as curve 2 (only scan 20 is shown). A well-defined redox couple is observed at the HHC|GelB|MH|Au electrode with a reductive peak potential of −0.018 V and a corresponding oxidative peak potential at 0.054 V. These redox reactions can be explained as the reduction and oxidation of the heme group present in the HHC protein [15–16]. The formal potential ($E^{\circ\prime}$) for the redox reaction of HHC is 0.018 V, consistent to the value of cytochrome *c* in solution [17]. A stability study showed that from scan 1 a stable electrochemical signal is obtained with no leakage of the protein into the HEPES cell solution indicating that the gelatin matrix forms a stable environment for the selected enzyme.

The fact that gelatin is an ideal microenvironment for HHC (heme group surrounded by different amino acids) can be explained by the biocompatibility, i.e. the presence of similar amino acids in the HHC protein as well as in the gelatin matrix. To prove this statement, 0.2 mmol L^{-1} $K_4Fe(CN)_6$ was entrapped in a gelB matrix instead of HHC. The heme group surrounded with amino acids (HHC) was thus replaced by a single iron ion, the compatibility of the amino acids is absent. In the first scan, an oxidation and reduction process is observed at respectively 0.212 and 0 V, corresponding to the $[Fe(CN)_6^{3-}]/[Fe(CN)_6^{4-}]$ redox reactions. The oxidation and reduction peak current decrease markedly as a function of scan number indicating a loss of $K_4Fe(CN)_6$ from the gelatin matrix into the cell solution. After 60 scans, there is no longer electrochemically active $K_4Fe(CN)_6$ present in the hydrogel. Compared to the experiment with HHC entrapped in a gelatin matrix, it is now clear that gelatin is not a suitable microenvironment for $K_4Fe(CN)_6$ because there is no amino acid interaction between $K_4Fe(CN)_6$ and gelatin.

A profound stability study showed that the HHC|GelB|MH|Au electrodes are stable as a function of time. The modified electrodes were kept in a air or in a HEPES buffer solution for 1 week. After that period, the stability was checked electrochemically and spectroscopically (UV–vis). Electrochemically, the peak current and the surface under the HHC-peak are quite stable for 1 week. Only a broadening of the peak is observed, probably indicating a small reorganization of the protein film or a change in protein conformation. When the prepared electrode was stored in solution, the stability of the film was checked by obtaining a UV–vis spectrum every day during 1 week. No HHC related signal was observed in that period, indicating that HHC in tightly entrapped in the gelatin matrix.

3.2. ATR-IR characterization of a HHC-gelatin modified electrode

The ATR-IR spectrum of the GelB|MH|Au electrode (Fig. 2(a)) shows four important characteristic regions (i.e. amide A, amide I, amide II and amide III bands) compared to a blank measurement (MH|Au, Fig. 2(c)). The amide A mode consists of bands at 3324 cm^{-1}, 2935 cm^{-1} and 2837 cm^{-1} which correspond to an NH stretch, coupled with hydrogen bonding, a CH_2 asymmetrical stretch and a CH_2 symmetrical stretch, respectively [18,19]. The amide I band, which is due primarily to C=O stretching of the peptide groups, is extremely sensitive to changes in the gelatin chain conformation. The wavenumbers of the characteristic bands of these carbonyl groups are determined by the local chemical environment and the degree of dipole–dipole interaction between neighbouring carbonyl groups [20]. Two characteristic bands can be distinguished within the amide I mode. The band at 1653 cm^{-1} is related to the presence of triple helices and β-turns while the band at 1638 cm^{-1} corresponds to random coils [20]. The amide II region consists of bands at 1550 cm^{-1} (i.e. NH bend coupled with CN stretch), 1450 cm^{-1} (i.e. CH_2 bend) and 1338 cm^{-1} (i.e. CH_2 wagging of praline) [21]. The final characteristic region is the amide III, which is composed of three characteristic bands. The band at 1168 cm^{-1} corresponds to an NH bend. The C–O stretch is responsible for the band at 1083 cm^{-1}, while the band at 1034 cm^{-1} is related to skeletal stretches [19,21]. The results indicate that ATR-IR spectroscopy is a suitable tool to demonstrate the presence of gelatin on the electrode surface. In addition, the technique enables to gain insight into the protein conformation on the surface. The latter is of relevance since the protein conformation significantly influences its biological activity.

The ATR-IR spectrum of the HHC|GelB|MH|Au electrode (Fig. 2(b)) shows a lot of similarities with the ATR-IR spectrum of the GelB|MH|Au electrode (Fig. 2(a)). The latter was anticipated based on the fact that both samples contain a significant amount of gelatin on their surface. In addition, HHC is also a protein composed of a large variety of amino acids connected via peptide linkages. However, several distinct differences can be distinguished when comparing both IR spectra. The band at 1450 cm^{-1} in the IR spectrum of the GelB|MH|Au sample is also present in the IR spectrum of the HHC|GelB|MH|Au sample. However, band widening can be observed together with the presence of a shoulder at higher wavenumbers. This can be attributed to HHC which is characterized by a band at 1456 cm^{-1}, as already indicated in a previous paper from our research group [22]. The band at 1168 cm^{-1} has shifted to 1175 cm^{-1} and its band width has become significantly higher. The shift of the band maximum and the higher band width are probably related to a conformational change of both proteins in the presence of one another since HHC shows a band maximum at 1161 cm^{-1} when present on the electrode without gelatin. Finally, additional bands at 1005 cm^{-1} and 950 cm^{-1} are observed in the ATR-IR spectrum of the HHC|GelB|MH|Au sample (Fig. 2(b)). These bands correspond with a conformational change

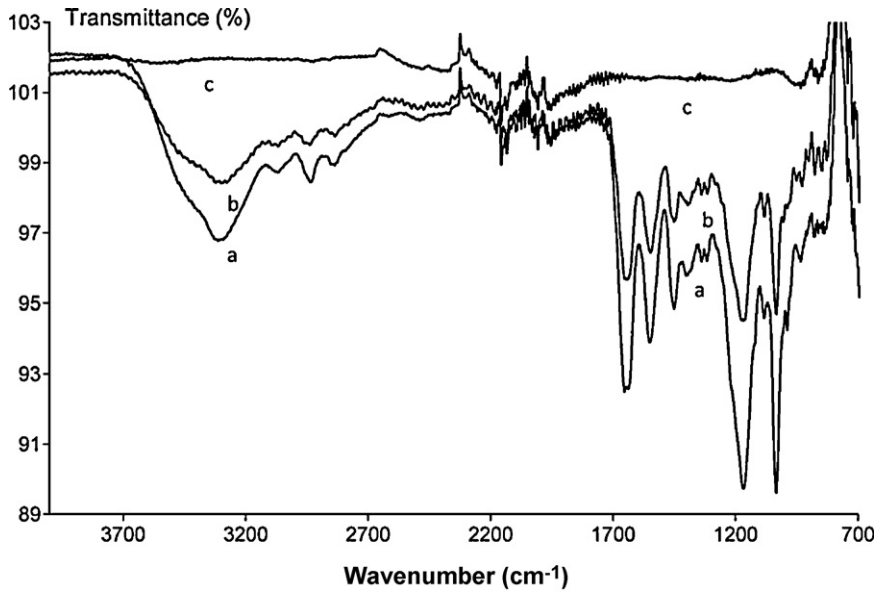

Fig. 2. ATR-IR spectra of GelB|Au (a), HHC|GelB|Au (b) and MH|Au (c).

of gelatin and/or with a conformational change of HHC. In the latter case, the bands of HHC have shifted from 1022 cm^{-1} and 962 cm^{-1} respectively. The obtained results are of relevance in view of potential biosensor applications, since changes in protein conformations have been reported to significantly affect their binding capacity [23]. As a result, the HHC conformation is important with respect to the incorporation of specific enzymes and/or proteins capable of detecting biochemical and/or physiological changes.

3.3. Determination of the thickness of a HHC-gelatin film by surface profilometry

The thickness of the HHC-gelatin film was determined using a 3D surface profiler. The thickness of semi-transparent films can be obtained by measuring the step height at the edge of the film or by measuring through the film to the substrate. In the latter case, the VSI technique is employed. Fig. 3 shows a film thickness plot of the electrode and indicates an average thickness of 23 μm. This relatively high value is the result of inter-protein as well as protein-gelatin cross-linking which occur on the electrode surface. The film thickness is affected by several parameters including the protein concentration applied, the immobilization strategy and the nature of the active gold surface. The layer thickness is of relevance since electron transfer from the 'sensing' enzyme or protein to the electrode should be retained upon incorporation in the HHC film. A second approach for determining the thickness by the optical profiler is making a hole in the gelatin film with a CO_2 laser and measuring the thickness of the film at the edge. Following this approach, one avoids the estimation of the index of refraction of the gelatin film. Results show that the thickness of the HHC-gelatin film is 22.7 μm.

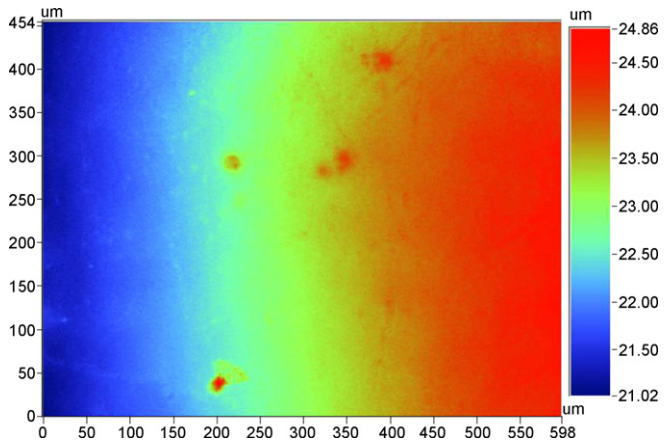

Fig. 3. Optical profilometry of a HHC|GelB(5 m%)|MH|Au electrode.

3.4. Influence of the HHC concentration and the scan rate on the electrochemical behaviour of HHC

In order to reveal the nature of the electrochemical process, the HHC concentration was varied in a first set of experiments. Fig. 4 shows the cyclic voltammetric behaviour of four HHC|GelB|MH|Au electrodes with different HHC concentration in a gelB matrix: 0.05 mmol L^{-1} (1); 0.1 mmol L^{-1} (2); 0.15 mmol L^{-1} (3) and 0.26 mmol L^{-1} (4). The same peaks were observed as in Fig. 1, only the peak current of the oxidation and reduction reaction changes: the higher the HHC concentration, the higher the peak

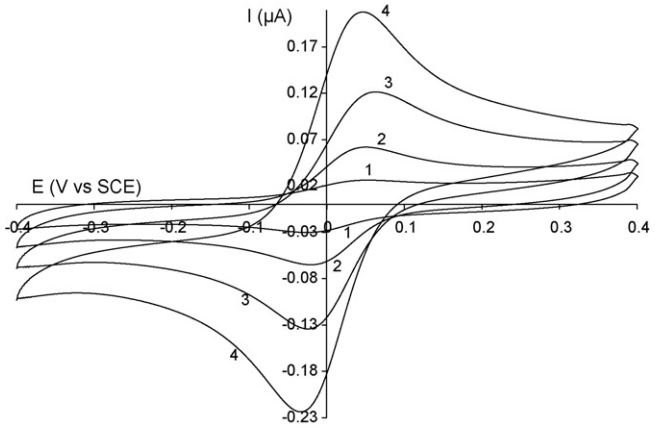

Fig. 4. The current potential behaviour of four HHC|GelB(5 m%)|MH|Au electrodes, in which the concentration of HHC is different: 0.05 mmol L^{-1} (1), 0.1 mmol L^{-1} (2), 0.15 mmol L^{-1} (3) and 0.26 mmol L^{-1} (4).

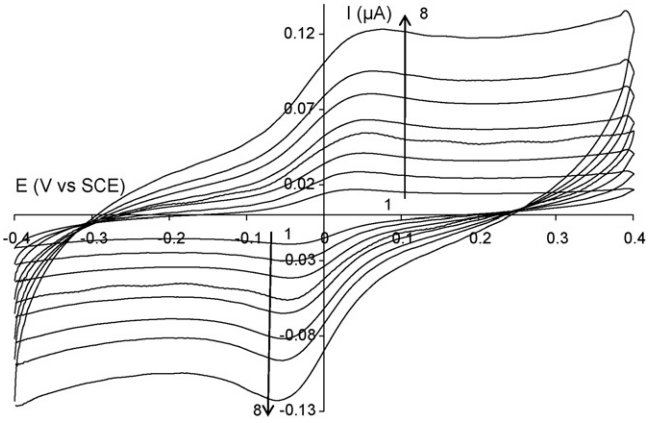

Fig. 5. The current potential behaviour of a HHC(0.11 mM)|GelB|MH|Au electrode in a 10 mmol L^{-1} HEPES pH 7 buffer solution at different scan rates: 10 mV s^{-1} (1), 25 mV s^{-1} (2), 50 mV s^{-1} (3), 75 mV s^{-1} (4), 100 mV s^{-1} (5), 150 mV s^{-1} (6), 200 mV s^{-1} (7) and 300 mV s^{-1} (8).

current. The relationship between the peak current and the HHC concentration is linear [24].

Secondly, the influence of the scan rate ν on the peak current I_p was investigated to determine the nature of the process. Fig. 5 shows the oxidation and reduction of HHC entrapped in a gelB matrix in a HEPES buffer solution over a wide range of scan rates. In the range of the explored scan rates, electron diffusion control is observed. The slope for both redox processes when plotting log I versus log scan rate is ca. 0.52, indicating a reaction of a particle in solution [24]. The proteins diffuse into the gelatin film in which they are entrapped, and the electron transfer process is achieved by exchange of electrons between the bound proteins. It could be calculated that for a film thickness of ca. 20 μm, diffusion controlled voltammetric responses are expected [25].

3.5. Influence of the mass% of GelB on the electrochemical behaviour of HHC

The influence of the mass percentage of gelB (in the range of 2.5–12.5 m/v%) on the electrochemical behaviour of HHC is shown in Fig. 6. The higher the mass percentage of GelB, the lower the oxidation and reduction peak current of HHC. A possible explanation for this phenomenon is the formation of physical entanglements (i.e. triple helix formation) within the gelatin hydrogel [26,27]. As a result, the hydrogel is physically cross-linked and the mobility

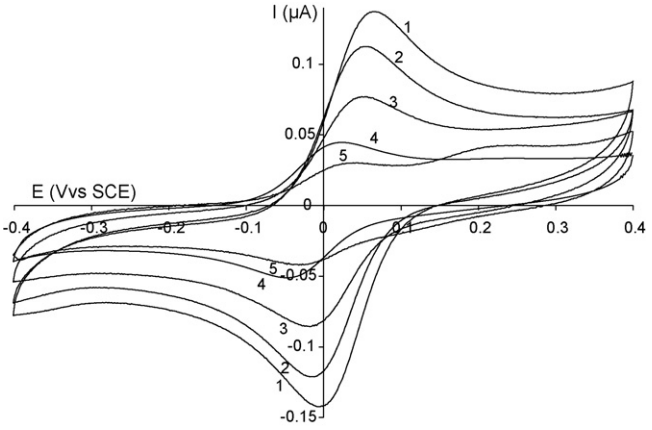

Fig. 6. The current potential behaviour of five HHC(0.14 mM)|GelB|MH|Au electrodes, in which the mass percentage of GelB is different: 2.5 m% (1), 5 m% (2), 7.5 m% (3), 10 m% (4) and 12.5 m% (5).

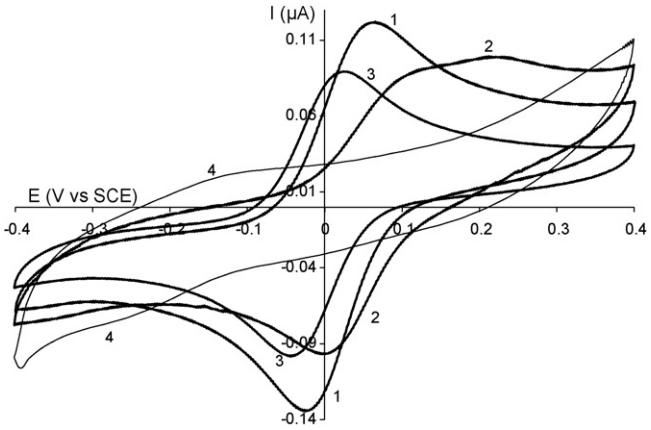

Fig. 7. The current potential behaviour of four HHC(0.14 mM)|Gel(5 m%)|MH|Au electrodes, in which the nature of gelatine is different: GelB (1), GelA (2), GelMOD (3) and GelSH (4).

of the HHC molecules embedded in the gelatin hydrogel is limited [28,29]. The latter is also seen in electrochemical data. At the highest percentage, one can observe two different oxidation reactions.

3.6. Influence of the nature of gelatin on the electrochemical behaviour of HHC

Fig. 7 represents the cyclic voltammetric behaviour of 0.5 mmol L^{-1} HHC entrapped in different types of gelatin immobilized on a gold electrode in a 10 mmol L^{-1} HEPES buffer solution. In the case of gelA, gelB and gelMOD, the gold surface was pretreated by immersing the electrode in a 1 mmol L^{-1} 6-mercaptohexanol solution for 18 h at room temperature, which allowed the adsorption of a SAM onto the surface (as is described in Section 2). For thiolated gelatin (gelSH), the gold surface was not modified in order to establish a covalent bonding between gold and the thiol groups present in the thiolated gelatin matrix [14]. The current potential behaviour of HHC present in a gelB matrix (curve 1) is described in detail in a previous paragraph (Fig. 1).

The iso-electric point of gelB has a value of ca. 5, which results in a negative charge of the gelB matrix at physiological pH. Because HHC carries a global positive charge, it is expected that gelB forms a more preferable environment for HHC compared to GelA which has a positive charge, as its iso-electric point is ca 8. Curve 2 shows the current potential behaviour of HHC encapsulated in a gelA matrix. A reversible redox behaviour is observed. Apparently, the peak height of the redox processes is lower and one can observe a deconvolution and potential shift of the oxidation process. This is probably due to the fact that GelA is a less attractive environment for HHC because of the lack of ionic interactions.

The voltammetric behaviour of HHC in gelMOD is shown in curve 3. GelMOD is characterized by the presence of crosslinkable methacrylamide moieties indicating a stable, environment for proteins. Indeed, a reversible redox couple is observed, comparable to the electrochemical behaviour of HHC in gelB. In gelMOD part of the amines of gelB are modified with methacrylamide side groups. GelMOD thus possesses less amine side chains than gelB able to form hydrogen bonds with HHC [30]. The latter is a likely explanation for the observed decrease in peak current. Thiolated gelatin was selected especially to obtain a covalent linking between the gold surface and the gelatin matrix. The corresponding electrochemical behaviour of HHC entrapped in a GelSH matrix is shown in curve 4. A pair of ill-defined redox processes is observed around −0.2 V. It seems that the heme related redox reactions are shifted towards more negative potentials sometimes indicating a denaturation of the protein. A possible explanation is the fact that the

thiolated gelatin does not completely cover the electrode surface. Therefore, the HHC is affected in a negative sense by the bare hydrophobic gold surface. Free spots of bare gold could be the reason for the denaturation of HHC. This will be investigated in more detail in the future. Based on the above results, the authors choose to select gelB as the most appropriate matrix for the immobilization of HHC.

4. Conclusions

This paper describes the electrochemical behaviour of HHC entrapped in a gelatin matrix immobilized on a gold surface. HHC was successfully immobilized into a gelatin network. The biocompatible hydrogel provides a favourable environment for HHC incorporation. A full electrochemical characterization of the polymeric film was made by studying different parameters such as HHC concentration, scan rate and the nature of the gelatin matrix. ATR-IR spectroscopy was used to prove the actual immobilization and enabled to gain insight into the protein conformation. This is of relevance is view of potential biosensor applications, since changes in protein conformations have been reported to significantly affect their binding capacity [23]. As a result, the HHC conformation is important with respect to the incorporation of specific enzymes and/or proteins capable of detecting biochemical and/or physiological changes.

References

[1] J.E. Eastoe, A.A. Leach, in: A.G. Ward, A. Courts (Eds.), The Science and Technology of Gelatin, Academic Press, New York, 1977 (Chapter 3).
[2] S.B. Lee, H.W. Jeon, Y.W. Lee, Y.M. Lee, K.W. Song, M.H. Park, Y.S. Nam, H.C. Ahn, Biomaterials 24 (2003) 2503–2511.
[3] P. Gupta, K. Vermani, S. Garg, Drug Disc. Today 7 (2002) 569–579.
[4] L.H. Lin, K.M. Chen, Colloids Surf. A: Physicochem. Eng. Aspects 272 (1–2) (2006) 8–14.
[5] P. Johns, A. Courts, The Science and Technology of Gelatin, Academic Press, New York, 1977.
[6] S. Oellerich, H. Wackerbarth, P. Hildebrandt, J. Phys. Chem. B 106 (2002) 6566–6580.
[7] J. Gong, P. Yao, H. Duan, M. Jiang, S. Gu, L. Chunyu, Biomacromolecules 4 (2003) 1293–1300.
[8] F.A. Armstrong, G.S. Wilson, Electrochim. Acta 45 (15–16) (2000) 2623–2645.
[9] Y. Wu, S. Hu, Microchim. Acta 159 (2007) 1–17.
[10] M. Fedurco, Coord. Chem. Rev. 209 (2000) 263–331.
[11] K. Miki, T. Ikeda, H. Kinoshita, Electroanalysis 6 (8) (1994) 703–705.
[12] W.R. Hagen, Eur. J. Biochem. 182 (1989) 523–530.
[13] A.I. Van Den Bulcke, B. Bogdanov, N. De Rooze, E.H. Schacht, M. Cornelissen, H. Berghmans, Biomacromolecules 1 (1) (2000) 31–38.
[14] S. Van Vlierberghe, K. De Wael, H. Buschop, A. Adriaens, E. Schacht, P. Dubruel, Macromol. Biosci. 8 (12) (2008) 1090–1097.
[15] R.S. Sirohi, M.A. Genshaw, J. Electrochem. Soc. 116 (1969) 910.
[16] H.A. Heering, F.G.M. Wiertz, C. Dekker, S. De Vries, J. Am. Chem. Soc. 126 (2004) 11103–11112.
[17] F. Hawkridge, T. Kuwana, Anal. Chem. 45 (7) (1973) 1021–1027.
[18] K.P. Sai, M. Babu, Comp. Biochem. Physiol. B: Biochem. Mol. Biol. 128 (1) (2001) 81–90.
[19] Y. Abe, S. Krimm, Biopolymers 11 (9) (1972) 1817.
[20] D.A. Prystupa, A.M. Donald, Polym. Gels Networks 4 (2) (1996) 87–110.
[21] M. Jackson, L.P. Choo, P.H. Watson, W.C. Halliday, H.H. Mantsch, Biochim. Biophys. Acta: Mol. Basis Dis. 1270 (1) (1995) 1–6.
[22] K. De Wael, S. Van Vlierberghe, H. Buschop, P. Dubruel, B. Vekemans, E. Schacht, L. Vincze, A. Adriaens, Surf. Interface Anal. 41 (5) (2009) 389–393.
[23] E. Keyhani, D. Minai-Tehrani, Biochim. Biophys. Acta: Bioenergetics 1506 (1) (2001) 1–11.
[24] M. Noel, K.I. Vasu, Cyclic Voltammetry and the Frontiers of Electrochemistry, Aspect Publications, London, 1990.
[25] K. De Wael, H. Buschop, L. De Smet, A. Adriaens, Talanta 76 (2008) 309–313.
[26] H.B. Bohidar, S.S. Jena, J. Chem. Phys. 100 (9) (1994) 6888–6895.
[27] H.B. Bohidar, S.S. Jena, J. Chem. Phys. 98 (11) (1993) 8970–8977.
[28] M. Zandi, H. Mirzadeh, C. Mayer, Iran. Polym. J. 16 (12) (2007) 861–870.
[29] C. Wu, W. Schrof, D. Lilge, E. Luddecke, D. Horn, Makromol. Chem.: Macromol. Symp. 40 (1990) 153–166.
[30] L. Muley, B. Baum, M. Smolinski, M. Freindorf, A. Heine, G. Klebe, D.G. Hangauer, J. Med. Chem. 53 (5) (2010) 2126–2135.